

Comparing the Differences in Brain Activities and Neural Comodulations Associated With Motion Sickness Between Drivers and Passengers

Kuan-Chih Huang¹, Alka Rachel John, Tzyy-Ping Jung², *Fellow, IEEE*, Wen-Feng Tsai, Yi-Hsin Yu, and Chin-Teng Lin³, *Fellow, IEEE*

Abstract—It is common to believe that passengers are more adversely affected by motion sickness than drivers. However, no study has compared passengers and drivers' neural activities and drivers experiencing motion sickness (MS). Therefore, this study attempts to explore brain dynamics in motion sickness among passengers and drivers. Eighteen volunteers participated in simulating the driving winding road experiment while their subjective motion sickness levels and electroencephalogram (EEG) signals were simultaneously recorded. Independent Component Analysis (ICA) was employed to isolate MS-related independent components (ICs) from EEG. Furthermore, comodulation analysis was applied to decompose spectra of interest ICs, related to MS, to find the specific spectra-related temporally independent modulators (IMs). The results showed that passengers' alpha band (8-12 Hz) power increased in correlation with the MS level in the parietal, occipital midline and left and right motor areas, and drivers' alpha band (8-12 Hz) power showed relatively smaller increases than those in the passenger. Further, the results also indicate that the enhanced activation of alpha IMs in the passenger than the driver is due to a higher degree of motion sickness. In conclusion, compared to the driver, the passenger experience more conflicts among multimodal sensory systems and demand neuro-physiological regulation.

Index Terms—Electroencephalography (EEG), motion sickness, independent component analysis (ICA), independent modulator, passenger, driver.

Manuscript received January 19, 2021; revised May 29, 2021; accepted June 17, 2021. Date of publication June 28, 2021; date of current version July 12, 2021. This work was supported in part by the Ministry of Science and Technology, Taiwan, under Contract MOST 108-2221-E-009-120-MY2 and Contract MOST 109-2221-E-009-050-MY2 and in part by the Australian Research Council (ARC) under Grant DP180100670, Grant DP180100656, and Grant DP210101093. (Corresponding authors: Kuan-Chih Huang; Chin-Teng Lin.)

This work involved human subjects in its research. Approval of all ethical and experimental procedures and protocols was granted by National Chiao Tung University under Application No. NCTU-REC-105-073.

Kuan-Chih Huang, Wen-Feng Tsai, and Yi-Hsin Yu are with the Brain Research Center, Department of Electrical and Computer Engineering, National Yang Ming Chiao Tung University, Hsinchu 30010, Taiwan (e-mail: kchuang.ece91g@nctu.edu.tw).

Alka Rachel John is with the Faculty of Engineering and IT, Australian Artificial Intelligence Institute, University of Technology Sydney, Ultimo, NSW 2007, Australia.

Tzyy-Ping Jung is with the Swartz Center for Computational Neuroscience, Institute for Neural Computation, University of California San Diego, La Jolla, CA 92093 USA.

Chin-Teng Lin is with the Faculty of Engineering and IT, Australian Artificial Intelligence Institute, University of Technology Sydney, Ultimo, NSW 2007, Australia, and also with the Brain Research Center, Department of Electrical and Computer Engineering, National Yang Ming Chiao Tung University, Hsinchu 30010, Taiwan (e-mail: chin-teng.lin@uts.edu.au).

Digital Object Identifier 10.1109/TNSRE.2021.3092876

This work is licensed under a Creative Commons Attribution 4.0 License. For more information, see <https://creativecommons.org/licenses/by/4.0/>

I. INTRODUCTION

MANY studies have studied motion sickness (MS), as it is a commonly experienced unpleasant disturbance in the sense of equilibrium during motion. According to the sensory conflict theory [1], the visual and vestibular system's conflicts during motion causes motion sickness. When information from different senses is not synchronously received, the brain attempts to resolve this conflict, and this situation may induce motion sickness. For instance, a traveler looks at a static book in the car, but the body feels dynamic movement. Meanwhile, the postural instability theory [2] speculates that postural control loss triggers motion sickness. Unexpected or unfamiliar actions can lead to a loss of control and the ability to maintain posture.

To create a sensory conflict situation, many previous studies have employed visual or vestibular stimulation or the coexistence of both, such as visual stimulation [3]–[5] or flow field videos [6], to incite motion sickness visually. To provoke motion sickness through motion, researchers have used rotational chair [7], or rotating circularvection drum [8] or an off-axis yaw oscillator [9]. In our previous study, motion sickness was induced by employing both visual and vestibular stimulation using a virtual driving environment [10], [11].

Many studies have explored the brain dynamics associated with motion sickness using electroencephalogram (EEG). Motion sickness provoked by a rotating drum is reflected by an increased frontal theta (4-7 Hz) power [12]. During a motion-sickness experiment where motion sickness was provoked by cross-coupled angular stimulation, increases in delta (1-3 Hz) and theta power were observed [13]. Increased delta power was also observed at the central electrodes, C3 and C4 during optokinetic rotating drum induced motion sickness [14]. However, in a virtual car driving experiment, theta power was negatively correlated to motion sickness [15]. In an experiment where motion sickness was induced by an object finding VR task, increases in the frontal and temporal delta and beta (13-30 Hz) power were found to be associated with motion sickness [16]. It is also reported that decreases in alpha (8-12 Hz) power reflect motion sickness induced by vestibular stimuli at the motor and parietal regions, broadband power increase at the midline occipital region and increases in delta and theta power at occipital regions [10].

Among all of the cited motion-sickness studies, the directions of EEG power changes were not consistent. This inconsistency might be due to the differences in the mechanism employed to provoke motion sickness. Some of the findings described above appeared simultaneously in different brain regions, but there was no more detailed discussion on why they occurred simultaneously.

The oscillations observed in the same frequency bands at different brain regions are from the simultaneous activation of EEG sources. Multiple neuromodulators influence different cortical areas to induce this co-oscillatory activity. In order to determine whether comodulatory processes influence the spectral response of independent EEG processes, researchers [17] have employed independent modulation analysis (IMA) after performing an independent component analysis (ICA). Temporally and spatially separate independent components (ICs) were derived from multichannel EEG data using the ICA method. IMA then applied a second ICA to decompose independent comodulatory systems that multiplicatively influence the spectra of independent components. That is, the second ICA separated the “spectral” synchronizations of distinct IC processes into independent modulators (IMs) [18]. The time series of these independent modulators were found to reflect the changes in alertness [18]. Thus IMA method may provide new insights on the brain dynamics of motion sickness.

In addition, researchers have explored the differences in motion sickness observed by passengers and drivers. Drivers are more resilient to motion sickness as they are in control of motion as compared to the passengers who have no control over the motion [19]. Another study used Simulator Sickness Questionnaire (SSQ) to evaluate the intensity of motion sickness (MS) in a driving video game. The drivers who drive the virtual vehicle reported lesser motion sickness symptoms as compared to passengers who watched the recordings of the game [20], [21]. Most past studies of the difference between passengers and drivers in motion sickness are based on questionnaires. However, no study has compared the changes in brain activity in motion sickness between drivers and passengers.

This study aims to explore differences in brain dynamic activities and motion sickness-related neural comodulations during motion sickness between passengers and drivers. We developed a VR-based motion-sickness platform with a wireless reporter that provides continuous and synchronous behavioral feedback during experiments along with a 64-channel EEG system to record the brain dynamics. The degree of motion sickness and EEG signals are recorded simultaneously. This platform employs both visual and vestibular stimuli to induce motion sickness, creating a realistic experimental paradigm. The recorded EEG signals were analyzed with ICA, time-frequency analysis and IMA to investigate motion sickness-related brain dynamics and neural comodulations.

II. MATERIALS AND METHODS

A. Participants

Fifteen males (mean age = 21.72; SD age = 2.29) and three females (mean age = 22; SD age = 0.82) were paid

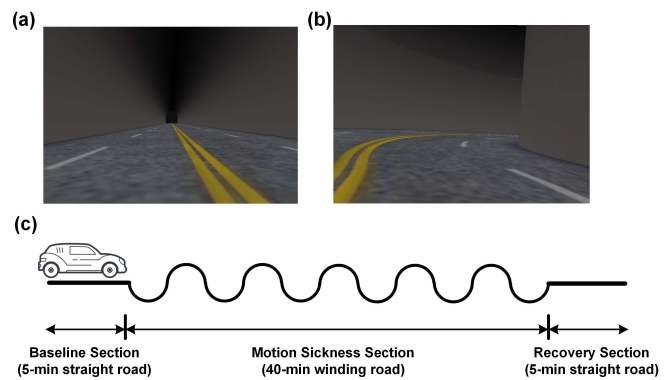


Fig. 1. Experimental scene. (a) a straight road and (b) a winding road and (c) the experimental paradigm. The experiment initially has five minutes on the initial straight road, which will be considered as the baseline. Then, motion sickness was induced by presenting winding roads for 40 minutes. After which, straight road is presented again for five minutes to afford some recovery from motion sickness.

to participate in this experiment. None of the participants reported any neurological or vestibular disorders. All participants had normal driving skills. Participants were informed that they might experience motion sickness (MS) in this experiment. The participants could end the experiment at any point of time if they felt a great rush of sickness, thus avoiding negative consequences. After an elaborate experiment description, all participants provided informed consent. In the end, eighteen pairs of yoked participants participated in this experiment.

B. Experimental Environment and Paradigm

1) *Experimental Environment*: Previous studies showed that driving simulators offers accurate and realistic driving experiences [22]–[25]. A high-fidelity and realistic virtual reality-based driving environment was constructed for this study. The system was coupled with seven similar PCs operating the same VR system, synchronized by LAN. The experimental environment was also comprised of a real car mounted on a motion platform with driver and passenger seats. Therefore, the system consists of three components: (1) a motion platform with six degree-of-freedom (DOF); (2) an actual car frame; and (3) seven LCD projectors projecting a 360-degree 3D VR scene. The conditions of the road and car dynamics influenced the movements of the platform. Fig. 1 shows the experimental environment of the VR-based dynamic motion platform. During the experiments, both the driver and the passenger wore a 64-channel EEG system and sat in the car for the motion sickness test. And participants continuously reported the degree of motion sickness they were feeling with a wireless device. The driver’s wireless device was embedded in the steering wheel. During the steering wheel’s operation, the driver could continuously report his degree of motion sickness by pushing embedded buttons. The passenger operated a wireless device to continuously report his degree of motion sickness. To induce motion sickness during the 3D tunnel VR scene, the depth of visual field was lessened, and visual distractors were removed.

2) *Experimental Protocol*: The experimental paradigm consists of three-stages, as shown in Fig. 1. The first stage consists of driving on a straight road for five minutes (Fig. 1a). This period will be taken as the baseline during EEG processing. In the second stage, motion sickness was induced by presenting a winding road (Fig. 1b) for 40 minutes. The subjects experienced sensory conflicts all the time in this stage. Motion sickness was induced using scenarios like making a right turn, which forces participants to the left side of the car, achieving a mismatch between visual input and the vestibular input to the brain. The road curvature and vehicle speed were randomly changed. Changes in driving speed and road conditions can easily induce motion sickness in subjects. In the third stage, in order to afford recovery from motion sickness, the participants were presented with a straight road for 5 minutes. The same group of subjects tested twice and took turns as passengers or drivers.

C. Motion Sickness Level and EEG Data Acquisition

In this study, the motion sickness induced brain dynamics were examined using the recorded EEG data and motion sickness levels. Instead of using a questionnaire to assess motion sickness, we collected the subjective ratings of motion sickness in real-time by asking the participant to adjust a sickness level bar ranging from zero to nine. Before the experiment, subjects had gone through a training session to become familiar with the steering wheel and wireless device operation and gave their consent for their participation. The conversation was prohibited during the experiment. The aim of this study was not informed to the participants. EEG data were obtained with Ag/AgCl electrodes combined with the highly conductive electrolyte gel (Quick-Gel, Neuromedical Supplies) that kept skin impedance below 5k Ω . NuAmps Express system was used to record the EEG data at a sampling rate of 500 Hz with a 32-bit quantization. Furthermore, 64-channel Quick-Caps manufactured by Compumedics NeuroScan were used in this research. All electrodes attached on both caps comply with the international 10-20 system [26], the electrode placement standard. Additionally, there are two reference channels (A1, A2) attached to the right and left mastoids.

D. EEG Data Processing

In this study, EEG data were analyzed and processed by MathWorks MATLAB (R2017a) and the EEGLAB Toolbox (version 14), an interactive MATLAB toolbox tailored to deal with EEG or MEG related data [27]. EEG channel locations were digitized by a 3-D digitizer and used by the advanced dipole fitting approach in the EEGLAB to visualize the source locations of the ICs. A 0.5 Hz high-pass filter was used on the recorded EEG data to eliminate the DC drift. After which, the high-frequency noise component was removed from the EEG data using a low-pass filtered at 50 Hz. Then to lower the computational load, the data was downsampled to 250 Hz. In order to remove the artifacts in the data from the eye and muscular activities, we used EEGLAB's automatic artifact rejection approaches enhancing the data's signal-to-noise ratio. Furthermore, we inspected the resultant

data using the EEGLAB visualization tool and eliminated the remaining contamination by hand. Finally, we applied independent component analysis to separate independent brain components from the high-density EEG data. The participants were monitored throughout the experiment to confirm that they were attentive to the experimental scenes. Then, all the preprocessed EEG data were used for further time-frequency analysis. In addition, the motion sickness ratings were synchronized with the each of these ICs' spectral changes over time. Then, the temporally and spectrally independent modulators (IMs) were discovered by performing ICA on the selected IC's reduced logarithmic spectra using principal component analysis (PCA).

E. Independent Component Analysis

EEG activities at each channel are a mixture of signals from multiple neuronal sources and nonbrain artifacts. ICA has been widely used to solve the blind source problem since the 1990s [28], and the results demonstrated that ICA is an effective method to separate the activities from distinct brain sources blindly. Additionally, ICA has been employed to remove artifactual components arising from eye blinks and muscular activities in the recorded EEG signal.

Mathematically, ICA is an algorithm that derives statistically independent non-Gaussian distribution from the multivariate EEG data. ICA assumes that (a) the distributions at each source activation is non-Gaussian; (b) the sum of the currents at each electrode is linear and there is nearly instantaneous signal conduction; and (c) the activations at different sources are temporally independent. ICA formulates this source separation problem as follows:

$$X = AS \quad (1)$$

$$U = WX \quad (2)$$

where X is a matrix of recorded scalp signals, A is called a mixing matrix, which is a linear transform, and S is a matrix of source activities. As shown in Equation (2), the ICA method derives U , the independent components activation matrix by computing W , also called the unmixing matrix which decomposes X , the recorded scalp data. The color-coded scalp maps are fashioned by projecting these independent source components (columns of W^{-1} , the inverse of the unmixing matrix) back to the channel data. The source of each independent component can be derived from their scalp map. For instance, the sources of eye activities are usually in the frontal region. The component related to muscle activity and other noises can be separated from the cortical source components.

We implemented the ICA method using 'runica' function from EEGLAB. For ICA, we limited the maximum number of steps for convergence to 1024, and the error was under 10^{-7} .

F. Time-Frequency Analysis

With scalp maps centralized in the frontal, central, left motor, right motor, parietal, occipital and occipital midline areas, seven independent components were selected for exploring the interactive brain dynamics during the experiment.

The spectral changes associated with motion sickness were determined based on the reported sickness level synchronized with the time series of the IC power spectra. Using a 500-points moving window with 50% overlap, the frequency responses of IC activations were computed. These epochs were subdivided into 125-point subwindows with 20% overlap. The power spectral density (PSD) was estimated with a 0.5 Hz resolution using a 512-point fast fourier transform (FFT), which was achieved by padding the subwindows with zeros. In order to compute the average power spectra over each two-second-long epoch, the power spectra were averaged over the corresponding subwindows. The decibel (dB) power was then computed from the resultant PSDs. As our data was resampled to 250 Hz and each window step was 250 Hz, the time series of the spectrum had a temporal resolution of 1 second.

G. Independent Modulator Decomposition

Previously, comodulatory processing mediating the spectral activities of independent cortical processes was examined by performing independent modulator analysis after the independent component analysis [17]. These independent modulators are temporally independent and fixed spectrally, offering a comprehensive picture of the neurological processes that define the overt behavioral responses. Specifically, a two-dimensional matrix was obtained by concatenating each component's time series of normalized power spectra. This matrix, X , is of size $[f \times c, t \times e]$ (where c represents the count of ICs; for each frequency bin, f represents the mean log-power spectra; t is the time series of each epoch; and e is the epoch count). PCA was employed to reduce X matrix to p components, transforming into a projection matrix, A and a matrix, S , with size $[p, t \times e]$; and $(AX = S)$. The selected component's spectral variations over time was decomposed by feeding the S matrix to the informax ICA algorithm. The informax ICA algorithm finds an unmixing matrix, W , such that $S = W^{-1}U$. U is the output matrix which consists of time courses of the activation of the independent modulators. Hence, the independent modulator analysis is devised as $AX = S = W^{-1}U$. Furthermore, $X = A^{-1}W^{-1}U$ if we derive A^{-1} , which is the pseudoinverse of eigenvector matrix, whose dimensions are reduced using PCA. For each independent modulator, the projection weight at all frequency bin of every component is specified by the columns of $A^{-1}W^{-1}$. The mean activation of each independent modulator over an epoch is provided by the matrix U , which holds the activations over $t \times e$.

In order to identify the independent modulators which were associated with motion sickness, Pearson's correlation coefficient was used to evaluate the correlation coefficients between the level of motion sickness and the time course of these independent modulators. We employed false discovery rate (FDR) to correct for multiple comparisons.

III. EXPERIMENTAL RESULTS

A. The Average Motion Sickness Level of Drivers and Passengers

In Fig. 2, the red and green curves represent the average motion sickness levels for the passenger and the driver,

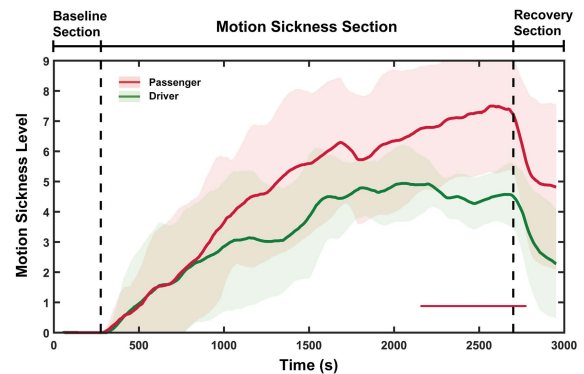


Fig. 2. The average trend and the distribution in subjective motion sickness level during the experiment. The red and green curves indicate the mean subjective motion sickness felt by passengers and drivers, respectively. The red and green areas along the mean subjective motion sickness levels are the standard deviations of motion sickness levels. The black vertical dotted lines indicate the start and end of the straight and winding roads. The red horizontal lines show significant differences between passengers' and drivers' motion sickness levels (Wilcoxon signed-rank test, $p < .05$).

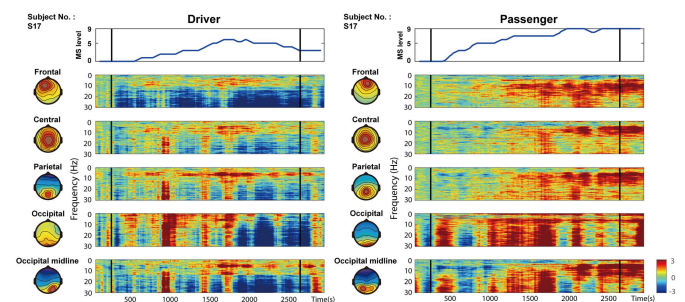


Fig. 3. Time course of the level of reported motion sickness and spectral power variations. A subject's reported level of motion sickness is shown in the top panel. The time-frequency responses relative to the baseline condition at the frontal, central, parietal, occipital and occipital midline components are shown in the other panel. The start and end of winding roads are indicated by black vertical lines in the figure. The relative spectral variations from the baseline is denoted by the color scale.

respectively, during the 50-minute experiment. The results indicated that the driver and the passenger suffered serious MS at the end of the experiment. Additionally, our results also demonstrate that the passenger's degree of motion sickness was higher than that felt by the driver. These results reflected that the passenger was more likely to feel motion sickness than the driver.

B. Time-Frequency Responses to Motion Sickness

1) *Time-Frequency Responses to Motion Sickness in Single Subject:* Figure 3 shows the time-frequency responses to the variations in the motion sickness level for the five selected independent components (frontal, central, parietal, occipital, and occipital midline components) from the same subject (Subject No. S17) playing different roles (driver/passenger). The experimental results revealed that the time-frequency responses of five independent components reflected the changes in MS, especially the spectral variations of passengers.

As shown in Fig. 3, the alpha power in several brain areas in both the passengers and drivers increased with the motion sickness level. Furthermore, the trends in alpha power

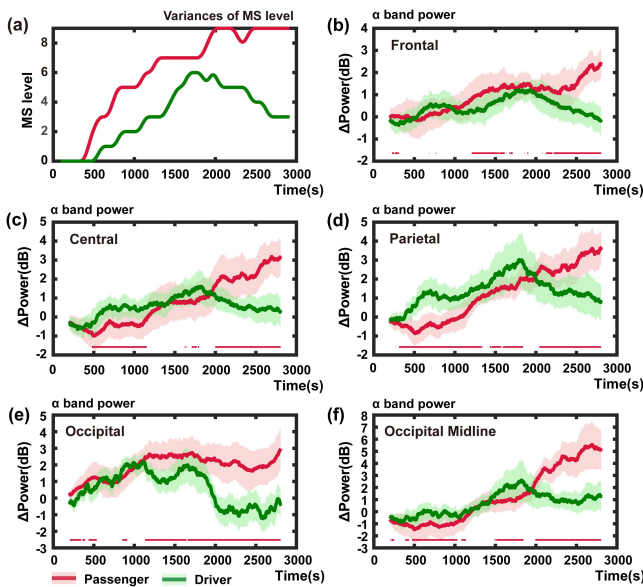


Fig. 4. Averaged alpha power and standard deviation with changes in MS levels (0 to 9) in the passenger and driver for the five components. (a) The averaged changes in MS levels in the passengers (red curve) and the drivers (green curve). (b)-(f) The effects of motion sickness on the observed spectra in the alpha band (8-12 Hz) were computed by removing the average baseline power (the first three-minute of experiment). In addition, the red and green distribution areas along the averaged alpha power changes are standard deviations of the passenger and driver alpha power, respectively. The red horizontal lines show significant differences in the averaged alpha power of the passenger and driver (Wilcoxon rank-sum test, $p < .05$).

are shown in Fig. 4. The result shows that alpha power increases as the motion sickness level rises. Furthermore, alpha power variations at the frontal, central, parietal, occipital, and occipital midline components were quite different between the passengers and drivers after spending 2000 s on the winding road.

2) Spectral Changes During Different Levels of Motion Sickness: The mean power spectra of the independent components under different levels of motion sickness (low, medium, high) is shown in Fig. 5. The green, blue, and red curves represent the first 3 minute of the low, medium, and high motion sickness levels, respectively, in the curved road section. The frequency bins where significant power variations were observed between high, medium and low motion sickness under the curved road driving condition were indicated by the red, blue and brown horizontal lines.

We compared the spectral changes in driving on a straight road and driving on the winding road. According to a previous study by Chen *et al.* [10], the passenger's alpha power would be suppressed in the parietal, motor, and occipital midline regions. In this study, the driver's alpha power showed the same phenomenon. Comparing the component power spectra under low, medium, and high motion sickness levels can reveal motion sickness-related spectral changes. Both the drivers' and passengers' alpha power increased as the motion sickness level rose. However, compared to the driver, the passenger's alpha power at the frontal, left motor, right motor, parietal and occipital midline regions increased more prominently with motion sickness levels. The alpha power of the passengers and

that of the drivers differ significantly at high sickness levels in the left motor and the occipital midline components, as shown in Fig. 5.

Despite the temporal independence of each component, the alpha activity of these components covaried both with each other and with the reported level of motion sickness. This finding indicates that there might be a comodulator or comodulators regulating the spectral activities in these brain areas characterized by ICs. In order to examine this possibility, we use IMA to analyze the spectral activations of the selected ICs in this study.

C. Motion Sickness-Related Independent Modulator Results

1) Results of Single-Subject Independent Modulator Decomposition: Figure 6 shows the results of the IMA for a single subject as a driver and a passenger. In the figures, a cell denotes the independent modulator's projection weights to the different ICs at different bins of frequency ranging from 1 to 50 Hz. Ten independent modulators were selected after applying PCA to reduce the dimensions. The mean projection weights for each independent modulator for frequency bin corresponding to delta (1-3 Hz), theta (4-7 Hz), alpha (8-12 Hz), beta (13-30 Hz) and gamma (31-50 Hz) bands were evaluated by adding the IM's projections on each component. Then, the independent modulator for each frequency band was determined by choosing the independent modulator with the greatest weight in that particular frequency band. The alpha modulators in Fig. 6a were IM2, IM5, IM6, IM8, IM9, IM10 and in Fig. 6b, it was IM1, IM3, IM4, IM5 and IM8 as they demonstrated significantly greater projection weights in the alpha activity across the brain. The results show that the number of alpha modulators is the highest among all passengers and drivers.

2) Cross-Subject Motion-Sickness-Related Independent Modulators Results: The correlation coefficients between the time courses of spectral amplitudes of each independent modulator and the motion sickness levels are shown in Table I. The statistically significant correlations are indicated by asterisks (*). The results indicate the dominance of alpha modulators on each IC's spectral changes. The correlation coefficients between all the independent modulators and motion sickness were significantly high, especially for the alpha ($r = 0.51 \pm 0.22$) modulators of passengers and drivers ($r = 0.49 \pm 0.18$).

3) Single-Subject Modulator Activation Results: The temporal dynamics of alpha independent modulator and the motion sickness levels for two subjects with different roles are shown in Fig. 7. With the increasing level of motion sickness, the alpha modulators activation increased.

4) Alpha Modulator Grouping Results: The alpha modulator activation in a representative subject across time is shown in Fig. 8. This section further investigates IM activations under different motion sickness levels across all the subjects. As each individual experienced/reported different maximal sickness levels, we first divided the entire session from each experiment into four categories: baseline (no sickness), low

TABLE I
CORRELATION COEFFICIENTS BETWEEN THE TIME COURSES OF SPECTRA OF IM AND THE MOTION SICKNESS LEVELS

Subjects No.	Drivers IMs					Passengers IMs				
	δ	θ	α	β	γ	δ	θ	α	β	γ
S01			0.41*		0.69*			0.46*		0.18*
S02			0.17*		0.42*	0.38*		0.18*	0.37*	
S03	0.27*	0.33*	0.5*	0.41*			0.19*	0.33*		0.44*
S04	0.21*		0.31*	0.37*				0.36*		0.26*
S05		0.41*	0.45*	0.16*	0.31*			0.52*		
S06		0.26*	0.67*	0.29*	0.32*			0.42*		0.57*
S07	0.51*		0.55*			0.49*	0.47*	0.73*	0.31*	0.3*
S08	0.56*		0.42*		0.38*		0.55*	0.31*	0.42*	
S09			0.73*		0.11*		0.24*	0.8*		0.57*
S10			0.83*		0.26*	0.11*		0.89*	0.43*	0.3*
S11			0.67*	0.43*	0.38*		0.3*	0.69*		0.31*
S12	0.2*		0.67*	0.22*	0.26*	0.49*		0.81*	0.66*	
S13	0.32*		0.2*	0.15*	0.3*	0.19*		0.24*		0.56*
S14	0.11*		0.32*		0.3*			0.21*	0.17*	0.5*
S15			0.74*		0.29*			0.75*		0.36*
S16		0.28*	0.36*					0.57*	0.35*	0.44*
S17			0.74*			0.48*		0.62*		
S18			0.41*	0.31*	0.45*		0.24*	0.55*		0.15*
Mean	0.37	0.32	0.5	0.29	0.34	0.36	0.33	0.52	0.39	0.38
STD	0.19	0.07	0.2	0.11	0.13	0.17	0.15	0.22	0.15	0.14

* denote significant correlations ($p < .05$).

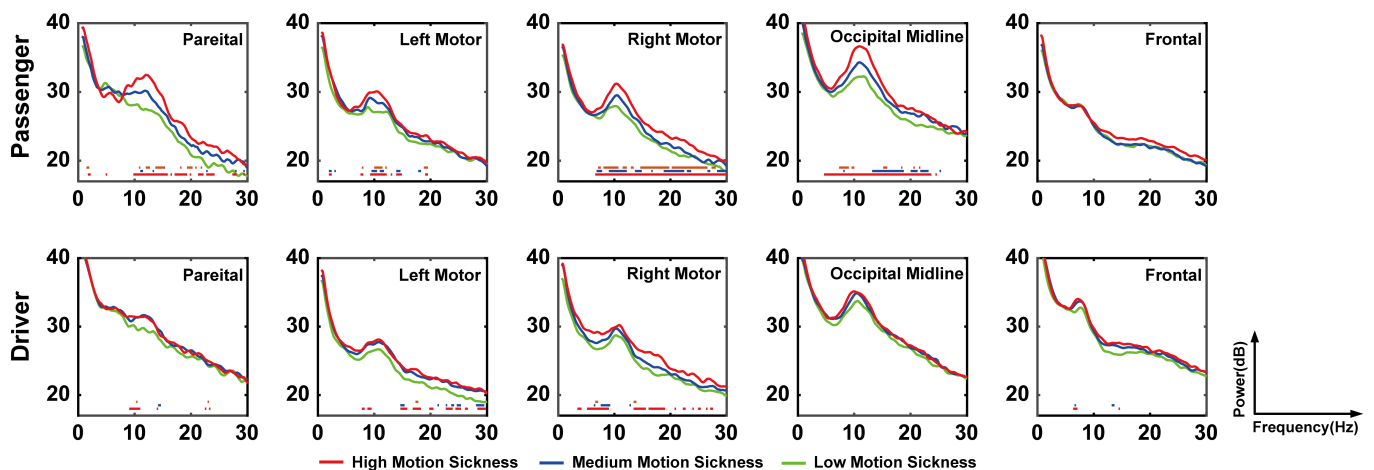


Fig. 5. Comparison of IC's power spectra of the passengers and the drivers under different levels of motion sickness. The mean power spectra of low, medium, and high sickness levels are shown in green, blue, and red curves, respectively. The red horizontal lines show significant variations in the average power spectra of high and low MS levels. The blue horizontal lines show significant changes in the power spectra of the medium and low MS levels. The brown horizontal lines show significant variation in the mean power spectra of the high and medium MS levels (Wilcoxon signed-rank test, $p < .05$).

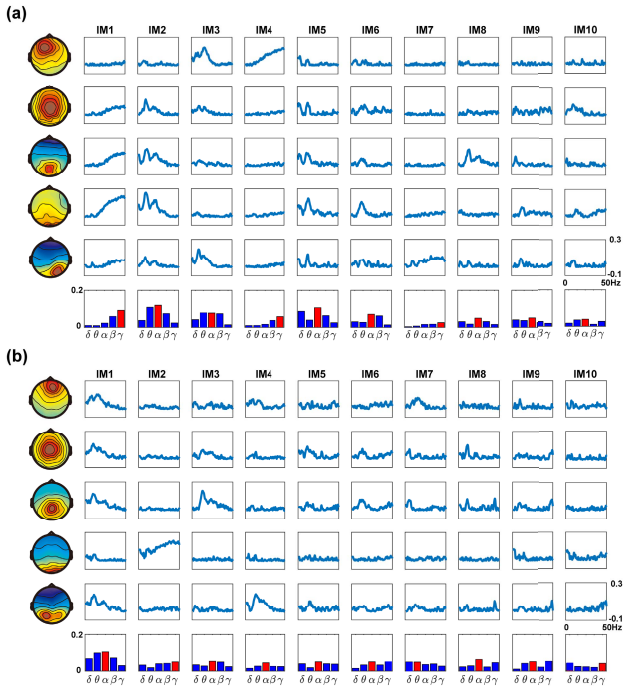


Fig. 6. A representative subject's estimated independent modulator processes as (a) the driver and (b) the passenger during the motion sickness study. The relative weight of projection from each independent modulator to different frequencies of each component, derived from a column of A-1W-1 is shown in each subplot. For every independent modulator, the modulator type is determined by the mean projection weights each frequency, which is shown at the bottom of the figure. The x-axis denotes the frequency (1 – 50 Hz) and the y-axis denotes the relative projection weights (–0.1 to 0.3).

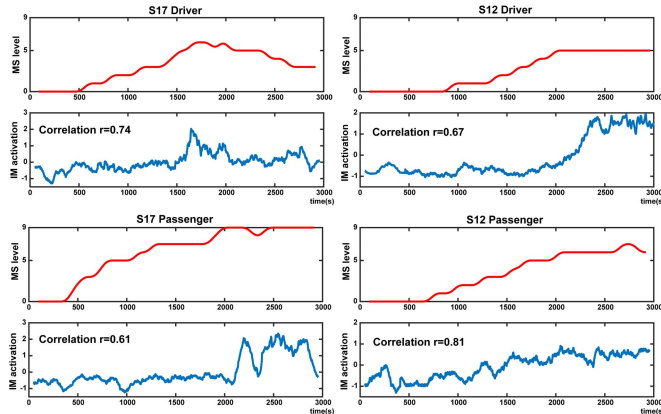


Fig. 7. Dynamics of MS and IM in drivers and passengers (Subjects 12 and 17). The top panel shows the time series of reported MS levels. The bottom panel shows the time course alpha modulator activation associated with MS.

motion sickness, medium motion sickness, and high motion sickness. The red asterisks in Fig. 8 indicate that the alpha IM activations differed significantly between passengers and drivers (Wilcoxon rank-sum test, $p < 0.05$). The orange asterisks in Fig. 8 indicate that the activations of the alpha IM differed significantly from low to high motion sickness in the passenger group. The blue asterisks in Fig. 8 indicate that the alpha IM activations differed significantly from low to high motion sickness in the driver group.

Figure 8 shows that the alpha IM activation increases significantly with the motion sickness level in both the drivers and

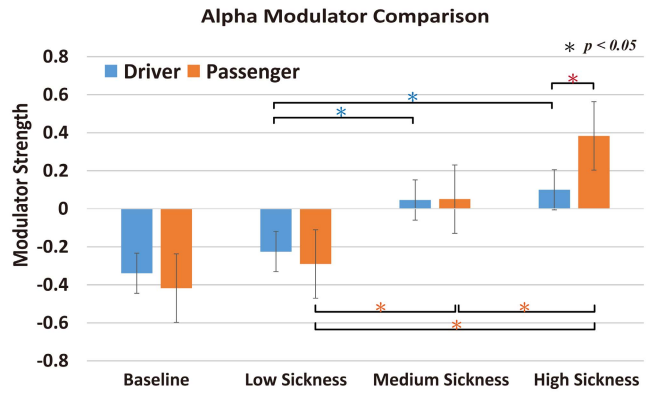


Fig. 8. Activations in the alpha IMs in passengers and drivers. The blue bars represent the driver group, and the orange bars represent the passenger group (Wilcoxon rank-sum test, $p < .05$).

passengers. Furthermore, the increase in the passenger's alpha IM activation is significantly higher than that of the driver's alpha IM in the high motion sickness condition.

IV. DISCUSSION

Previous studies have assumed that to suppress symptoms of MS, the best behavioral course of action is to align visual, vestibular and other sensory receptor information [29]. However, this alignment seems insufficient for explaining why the passenger is more prone to suffer from MS than the driver, even though both are receiving the same visual and motion inputs. To understand more about dynamic brain differences between the driver and the passenger in terms of MS, several MS experiments were conducted, and the experimental results from behavioral and EEG power spectra analysis are discussed. Our results further elucidate the neural comodulatory activities in motion sickness between passengers and drivers. In order to investigate the modulators of the neural dynamics associated with motion sickness in drivers and passengers, independent modulator decomposition was employed on the spectral changes of selected components. The alpha modulators significantly regulated the spectral activities of multiple ICs. In the experimental results, activations in alpha modulators positively reflected the MS levels, along with the subjective reports of passengers and drivers.

A. Subjective Levels of MS

The experimental results demonstrated that the motion sickness levels of the passengers were more severe than those of the drivers. This finding is consistent with previous studies, in which driver subjects who have control over the motion are less susceptible to motion sickness than passenger subjects who have no control over the motion [19]. Based on experiences of ordinary people, the driver rarely gets severe MS. However, this result also showed that both the driver and passenger suffered severe MS at the end of the experiment. It is reasonable to believe that the driver's acute MS may come from theatre sickness.

B. Motion Sickness Related Time-Frequency Responses

As shown in Fig. 5, we found that the spectral power of a passenger increases more than that of a driver. This result

might indicate that passengers are more susceptible to MS than drivers, quickly feeling dizziness, sweating, and other MS symptoms. In addition, the passenger have significantly greater overall spectral power as compared to the drivers, and the alpha band spectral power increases as the motion sickness level rises. The experimental result shows that whether in a passenger or a driver, alpha power is the EEG marker associated with motion sickness.

From the standpoint of spectral change occurring in different motion sickness levels, we found that when the passengers enter the winding road portion of the experiment from the straight road, there is alpha suppression in the left motor, right motor, parietal, and occipital midline components, as shown in Fig. 3. This result is consistent with a previous study that reported that somatic sensations from the movement of the platform are reflected in the brain networks [10]. Cheron *et al.* also reported that in a gravitational experiment, when the influence of gravity was eliminated, increases in oscillations at 10 Hz was observed at the sensorimotor and parieto-occipital regions [14]. They have reasoned that parietal region might be responsible for integrating information from different senses like vestibular input as it is located between the motor and somatosensory cortex. In our study, we also found that alpha power in the passenger in the left motor, right motor, parietal, and occipital midline components increased significantly as the MS level increased (*cf.* Fig. 3).

C. Comodulatory EEG Activity Covaries With Motion Sickness

Several previous studies reported that the cortical and thalamic activations may be modulated by neurotransmitters, like serotonin, dopamine, norepinephrine or acetylcholine. The impact of thalamic and cortical projections are explored in the possibility of comodulation [30]–[33]. Thalamus forms a thalamocortical network that receives sensory inputs from lower-level brain areas and projecting to a higher-order brain area [34]. The power spectral synchrony between different brain regions is known to be modulated by thalamic neurons [35], [36]. Consequently, the attentional resource allocation and synchronization across cortical areas might be mediated by neural modulator, which serves as an administrative control center. As the results demonstrate comparable spectral variations in the frontal, central, left motor, right motor, parietal, occipital midline and occipital components, it indicates that the deep brain is projecting to signals to the cortical areas. Cortical synchrony and oscillations associated with cognitive processes and information transmission might be influenced by this internal deep brain mechanism [37].

Sensory processing is reflected in the alpha activity. Integration of oscillations in the multimodal sensory systems are reflected by the synchronization of alpha power. Intricate brain computations and the integration of different brain regions are reflected in the alpha rhythm. Furthermore, postural instability, an initial symptom that generally precedes the onset of motion sickness, can also be accounted by the alpha power. In our previous studies, we noted that motion sickness is associated with the alpha power in the somatosensory area.

Therefore, the onset of motion sickness related to postural instability can be predicted by the peak of alpha independent modulator activation, that is observed to precede the maximum motion sickness (refer Fig. 7). While subjects were driving through winding roads, there might have been conflicts among various sensory inputs, which leads to an increase in top-down processing in high demand states, resulting in the observed alpha synchronization. Our findings also demonstrate spectral changes observed in the independent components are mediated by the alpha modulators. Moreover, the levels of motion sickness was positively correlated with the activation of alpha modulators in both driver and passenger groups in Figs. 7 and 8. Fig. 8 shows that both the passenger and driver groups show a significant increase in alpha IM activation as the motion sickness level rises, albeit the alpha IM activation only increases slightly. These findings suggest that alpha modulation could be an indicator of MS to help regulate the dynamic activity of the cortex. However, in Fig. 8, alpha modulator activation in the passenger was significantly higher than that in the driver at high sickness levels.

D. Limitations

Although the current study results validated differences between the passenger and driver in brain dynamic activities and motion sickness-related neural comodulations during motion sickness, it is still important to keep in mind that the current result still has some limitations.

First, each subject conducted the MS experiment as the driver and passenger on different days. However, even the same individual, there are still slight differences in the basic physiological state on different days.

Second, although the study has yielded consistent results across the subjects as the driver and passenger in these experiments, more relevant factors, such as each subject's driving experience and habits, were still needed to perfect this study.

V. CONCLUSION

This study explores differences in brain dynamics that accompany fluctuations in the level of MS in drivers and passengers in a realistic driving task. In general, subjective behavioral reports showed the following: (1) when entering the winding course, the passenger was more susceptible to MS than the driver, and (2) the symptoms of MS in the passenger were also more severe than those in the driver. In addition, the analysis results show that MS-related spectral changes occur in multiple independent components, especially in alpha band power. The passenger's broadband power increases significantly more than the driver's spectral power. Time-frequency analysis suggested the comodulatory nature of the time courses of independent components. More specifically, independent modulators regulate the spectral variations in various brain areas. The independent modulator decomposition was thus applied on the temporally independent components' spectra to compare the differences in the activation of modulators between drivers and passengers. In our simulated driving experiments, both passengers and drivers exhibited

alpha suppression when they first entered the winding road, and then, the alpha power of the passengers increases significantly as they experience motion sickness. Study results show that the alpha augmentation of the passengers is higher than that of the drivers in the high sickness section of the driving experiment.

REFERENCES

- [1] J. T. Reason and J. J. Brand, *Motion Sickness*. New York, NY, USA: Academic, 1975.
- [2] G. E. Riccio and T. A. Stoffregen, "An ecological theory of motion sickness and postural instability," *Ecol. Psychol.*, vol. 3, no. 3, pp. 195–240, Sep. 1991.
- [3] B.-C. Min, S.-C. Chung, Y.-K. Min, and K. Sakamoto, "Psychophysiological evaluation of simulator sickness evoked by a graphic simulator," *Appl. Ergonom.*, vol. 35, no. 6, pp. 549–556, Nov. 2004.
- [4] N. Sugita *et al.*, "Evaluation of the effect of visually-induced motion sickness based on pulse transmission time and heart rate," in *Proc. SICE Annu. Conf.*, vol. 3, 2004, pp. 2473–2476.
- [5] H. Ujike, T. Yokoi, and S. Saida, "Effects of virtual body motion on visually-induced motion sickness," in *Proc. 26th Annu. Int. Conf. IEEE Eng. Med. Biol. Soc.*, Sep. 2004, vol. 1, pp. 2399–2402.
- [6] C. Strychacz, E. Viirre, and S. Wing, "The use of EEG to measure cerebral changes during computer-based motion-sickness-inducing tasks," *Proc. SPIE*, vol. 5797, pp. 139–148, May 2005.
- [7] T. Russomano *et al.*, "Development and validation of an electrically controlled rotatory chair to be used as a simulator for spatial disorientation and motion sickness," in *Proc. 25th Annu. Int. Conf. IEEE Eng. Med. Biol. Soc.*, Sep. 2003, vol. 4, pp. 3306–3308.
- [8] M. J. Williamson, M. J. Thomas, and R. M. Stern, "The contribution of expectations to motion sickness symptoms and gastric activity," *J. Psychosomatic Res.*, vol. 56, no. 6, pp. 721–726, 2004.
- [9] S. J. Wood, "Human otolith-ocular reflexes during off-vertical axis rotation: Effect of frequency on tilt-translation ambiguity and motion sickness," *Neurosci. Lett.*, vol. 323, no. 1, pp. 41–44, 2002.
- [10] Y. C. Chen *et al.*, "Spatial and temporal EEG dynamics of motion sickness," *NeuroImage*, vol. 49, no. 3, pp. 2862–2870, Feb. 2010.
- [11] C.-T. Lin, S.-F. Tsai, and L.-W. Ko, "EEG-based learning system for online motion sickness level estimation in a dynamic vehicle environment," *IEEE Trans. Neural Netw. Learn. Syst.*, vol. 24, no. 10, pp. 1689–1700, Oct. 2013.
- [12] S. Q. Hu, K. A. McChesney, K. A. Player, A. M. Bahl, S. B. Buchanan, and J. E. Scozzafava, "Systematic investigation of physiological correlates of motion sickness induced by viewing an optokinetic rotating drum," *Aviation Space Environ. Med.*, vol. 70, no. 8, pp. 759–765, Aug. 1999.
- [13] W. E. Chelen, M. Kabrisky, and S. K. Rogers, "Spectral analysis of the electroencephalographic response to motion sickness," *Aviation Space Environ. Med.*, vol. 64, no. 1, pp. 24–29, Jan. 1993.
- [14] G. Cheron *et al.*, "Effect of gravity on human spontaneous 10-Hz electroencephalographic oscillations during the arrest reaction," *Brain Res.*, vol. 1121, no. 1, pp. 104–116, Nov. 2006.
- [15] R. Hyman, "Stimulus information as a determinant of reaction time," *J. Exp. Psychol.*, vol. 45, no. 3, p. 188, 1953.
- [16] Y. Y. Kim, H. J. Kim, E. N. Kim, H. D. Ko, and H. T. Kim, "Characteristic changes in the physiological components of cybersickness," *Psychophysiology*, vol. 42, no. 5, pp. 616–625, 2005.
- [17] J. Onton and S. Makeig, "High-frequency broadband modulations of electroencephalographic spectra," *Frontiers Hum. Neurosci.*, vol. 3, p. 61, Dec. 2009.
- [18] S.-W. Chuang, L.-W. Ko, Y.-P. Lin, R.-S. Huang, T.-P. Jung, and C.-T. Lin, "Co-modulatory spectral changes in independent brain processes are correlated with task performance," *NeuroImage*, vol. 62, no. 3, pp. 1469–1477, Sep. 2012.
- [19] A. Rolnick and R. E. Lubow, "Why is the driver rarely motion sick? The role of controllability in motion sickness," *Ergonomics*, vol. 34, no. 7, pp. 867–879, 1991.
- [20] R. S. Kennedy, N. E. Lane, K. S. Berbaum, and M. G. Lillenthal, "Simulator sickness questionnaire: An enhanced method for quantifying simulator sickness," *Int. J. Aviation Psychol.*, vol. 3, no. 3, pp. 203–220, 1993.
- [21] X. Dong, K. Yoshida, and T. A. Stoffregen, "Control of a virtual vehicle influences postural activity and motion sickness," *J. Exp. Psychol., Appl.*, vol. 17, no. 2, p. 128, 2011.
- [22] J. Hoskovec and J. Štikar, "Training of driving skills with or without," *Stud. Psychol.*, vol. 34, no. 2, p. 183, 1992.
- [23] N. Galley, "The evaluation of the electrooculogram as a psychophysiological measuring instrument in the driver study of driver behaviour," *Ergonomics*, vol. 36, no. 9, pp. 1063–1070, Sep. 1993.
- [24] E. R. Hoffmann and R. G. Mortimer, "Drivers' estimates of time to collision," *Accident Anal. Prevention*, vol. 26, no. 4, pp. 511–520, 1994.
- [25] W. Schiff, W. Arnone, and S. Cross, "Driving assessment with computer-video scenarios: More is sometimes better," *Behav. Res. Methods, Instrum., Comput.*, vol. 26, no. 2, pp. 192–194, 1994.
- [26] P. Malmivuo, J. Malmivuo, and R. Plonsey, *Bioelectromagnetism: Principles and Applications of Bioelectric and Biomagnetic Fields*. New York, NY, USA: Oxford University Press, 1995.
- [27] E. R. Delorme and S. Makeig, "EEGLAB: An open source toolbox for analysis of single-trial EEG dynamics including independent component analysis," *J. Neurosci. Methods*, vol. 134, no. 1, pp. 9–21, Mar. 2004.
- [28] A. Bell and T. Sejnowski, "An information maximization approach to blind separation and blind deconvolution," *Neural Comput.*, vol. 7, pp. 1129–1159, Nov. 1995.
- [29] F. Schmääl, "Neuronal mechanisms and the treatment of motion sickness," *Pharmacology*, vol. 91, nos. 3–4, pp. 229–241, 2013.
- [30] T. W. Robbins, "Arousal systems and attentional processes," *Biol. Psychol.*, vol. 45, nos. 1–3, pp. 57–71, Mar. 1997.
- [31] M. T. Bardo, "Neuropharmacological mechanisms of drug reward: Beyond dopamine in the nucleus accumbens," *Crit. Rev. Neurobiol.*, vol. 12, nos. 1–2, pp. 37–68, 1998.
- [32] D. A. McCormick and T. Bal, "Sleep and arousal: Thalamocortical mechanisms," *Annu. Rev. Neurosci.*, vol. 20, no. 1, pp. 185–215, Mar. 1997.
- [33] B. S. Oken, M. C. Salinsky, and S. Elsas, "Vigilance, alertness, or sustained attention: Physiological basis and measurement," *Clin. Neurophysiol.*, vol. 117, no. 9, pp. 1885–1901, Sep. 2006.
- [34] S. M. Sherman and R. W. Guillery, *Exploring the Thalamus and Its Role in Cortical Function*. Cambridge, MA, USA: MIT Press, 2006.
- [35] D. Swick, J. A. Pineda, S. Schacher, and S. L. Foote, "Locus coeruleus neuronal activity in awake monkeys: Relationship to auditory P300-like potentials and spontaneous EEG," *Exp. Brain Res.*, vol. 101, no. 1, pp. 86–92, Sep. 1994.
- [36] S. Herculano-Houzel, M. H. J. Munk, S. Neuenschwander, and W. Singer, "Precisely synchronized oscillatory firing patterns require electroencephalographic activation," *J. Neurosci.*, vol. 19, no. 10, pp. 3992–4010, May 1999.
- [37] Y. B. Saalman, "Intralaminar and medial thalamic influence on cortical synchrony, information transmission and cognition," *Frontiers Syst. Neurosci.*, vol. 8, p. 83, May 2014.